THE FLOW STRUCTURE IN A THREE-DIMENSIONAL MODEL OF ABDOMINAL AORTIC BIFURCATION: ULTRASONIC AND NUMERICAL STUDY

D.E. Sinitsyna, A.D. Yukhnev, D.K. Zaitsev, M.V. Turkina

Peter the Great St. Petersburg Polytechnic University, St. Petersburg, Russian Federation

A numerical and experimental research of fluid flow structure on a model involving statistical-average bifurcations of the abdominal aorta and iliac arteries with an axisymmetric stenosis in the right common iliac artery has been conducted. It was shown that a two-vortex flow formed in the external iliac artery transforms a downstream into a four-vortex flow. The stenosis in the common iliac artery leads to formation of a recirculation zone behind it, namely, at the inner wall of the vessel. The following spatial bend of the external iliac artery leads to generation of a swirling flow in this vessel. A transitional flow, from a two-vortex to a single-vortex motion, forms in the internal iliac arteries.

Keywords: abdominal aorta's bifurcation, spatial bending of vessel, stenosis, ultrasound Doppler method

УЛЬТРАЗВУКОВОЕ И ЧИСЛЕННОЕ ИССЛЕДОВАНИЕ СТРУКТУРЫ ТЕЧЕНИЯ В ТРЕХМЕРНОЙ МОДЕЛИ БИФУРКАЦИИ БРЮШНОЙ АОРТЫ

Д.Э. Синицына, А.Д. Юхнев, Д.К. Зайцев, М.В. Туркина

Санкт-Петербургский политехнический университет Петра Великого,

Санкт-Петербург, Российская Федерация

Проведено расчетно-экспериментальное исследование структуры стационарного течения жидкости на модели, включающей среднестатистические бифуркации брюшной аорты и подвздошных артерий с осесимметричным стенозом в правой общей подвздошной артерии. Показано, что в наружной подвздошной артерии сначала формируется двухвихревое течение, которое далее, вниз по потоку, трансформируется в течение с четырьмя вихрями. Наличие гемодинамически значимого стеноза в общей подвздошной артерии приводит к формированию за ним отрывной зоны у внутренней стенки сосуда. Следующий за ним пространственный изгиб наружной подвздошной артерии приводит к генерации в ней закрученного течения. Во внутренних подвздошных артериях формируется переходное течение - от двухвихревого к одновихревому.

Ключевые слова: бифуркация брюшной аорты, пространственный изгиб сосуда, стеноз, ультразвуковой доплеровский метод

Introduction

The abdominal aorta is one of the most important arteries supplying blood to abdominal structures and lower limbs. Aortic occlusion is a common disease of the abdominal aorta occurring near the aortic bifurcation and damaging the surrounding organs, so it requires surgical treatment. Detailed analysis of the structure of flow in this segment of the vascular bed can provide insights into possible locations and causes of pathologies, uncovering data on the exit conditions necessary for simulation of blood flow in femoral arteries downstream.

First studies on flow structure in the abdominal aortic bifurcation were carried out in the 1980s. An experimental study in [1] considered a simplified model of aortic bifurcation, comparing it with with clinical measurements at rest. Velocity profiles in vessels of this model were recorded using magnetic resonance imaging at a Reynolds number Re = 1150. This number is estimated by the average flow rate at the time of maximum flow and by the inlet diameter of the vessel.

Ref. [2] was dedicated to numerical simulation of pulsatile flow in a simplified model of abdominal aortic bifurcation without spatial bends. The sizes of separated regions in the common iliac arteries were considered in two states: at Re = 702 for the resting case and at Re = 1424 for mild exercise (the Reynolds number was estimated by the mean flow velocity averaged over the cardiac cycle and the vessel's inlet diameter).

Generally, different configurations of simplified models of the given region were discussed in literature [2−4]. Flow structure in subsequent bifurcations of iliac arteries was not considered in most cases.

Numerical simulation using patient-specific models based on clinical measurements of the patient's blood vessel geometry is currently the focus of much attention [5, 6]. A number of studies use models with average geometry [7]. However, there are virtually no studies using average models of abdominal aortic bifurcation and subsequent iliac bifurcations; it would prove important to simulate these arteries based on averaged geometry of several groups of patients.

The focus is typically on regions with low shear stresses, associated with formation and development of atherosclerosis, as well as on the effect of wall elasticity on flow structure. For example, it was confirmed in [5] that wall elasticity only insignificantly affects the flow pattern, and the difference in averaged shear stresses in the 'rigid' and 'elastic' simulations does not exceed 10%. Therefore, rigid vessel models can be used as a first approximation in experimental studies [8].

To date, Doppler ultrasound is the most common clinical method for diagnosing blood flow, as it is relatively cheap, non-invasive and easy to use. Ultrasound imaging of the vortex structure of blood flow in vessels with complex spatial configuration opens up new opportunities for doctors, serving to improve the diagnostics of vascular pathologies. Numerical simulation carried out for laminar flow yields detailed information on the velocity fields, making it possible to interpret complex ultrasonic images [9].

This study considers flow structure using a model of the averaged abdominal aortic bifurcation and subsequent iliac bifurcations using the ultrasonic Doppler method and numerical simulation. The study includes analysis of the effect of stenosis in the common iliac artery on the flow structure.

Model of abdominal aortic bifurcation and subsequent bifurcations of the common iliac arteries

The model of the statistically average configuration of abdominal aorta and iliac arteries used in this study was constructed using averaged clinical data [10−15]. This developed model takes into account the characteristic spatial curvature of the vascular region with three bifurcations.

The model includes an outlet segment of the abdominal aorta with a diameter of 18 mm, which is divided into the right and left common iliac arteries with the diameter $D = 10.8$ mm (Fig. 1).

The common iliac arteries, in turn, are divided into external (diameter of 9.0 mm) and internal (diameter of 5.5 mm) iliac arteries. The total length of the aortic model is 215 mm.

Deviations from the axis of the outlet segment of the abdominal aorta are 20º for the left common illiac artery and 25º for the right one.

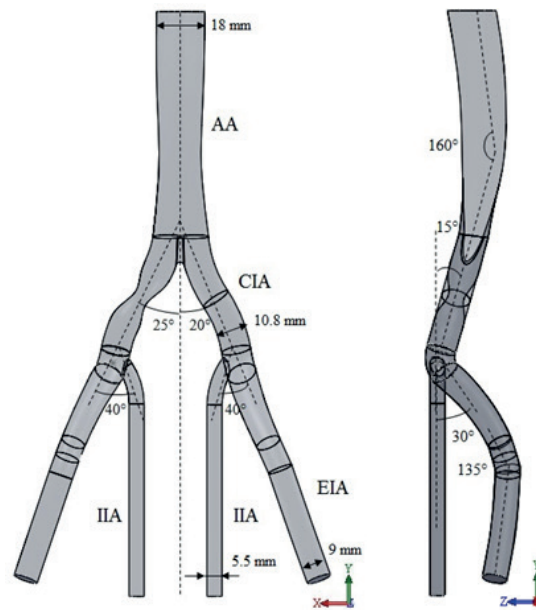The angle between the internal and external iliac arteries is 30º (side view) and 40º (front view).

Fig. 1. Model of average bifurcation of abdominal aorta and iliac arteries:
abdominal aorta AA, common iliac arteries CIA,
external iliac arteries EIA, internal iliac arteries IIA

The angle between the axis of the abdominal aorta and the plane of the common iliac arteries is 160º.

Hemodynamically significant axisymmetric stenosis is located in the right common iliac artery; its length is $L_s = 22$ mm, drift diameter $D_s = 5.9$ mm. The stenosis index (by area)

$$\text{STI} = (1 - D_s^2/D^2)\cdot 100\% = 70\%.$$

The variation of the radius R of the vessel in the stenosed region along the vessel axis is given by the formula:

$$R = 0.5D_s + 0.5(D - D_s)\cos^2(\pi y/L_s),$$
$$- L_s/2 \le y \le L_s/2.$$

Since bifurcation of the abdominal aorta is almost symmetric (there is only a slight difference in the deviation angles of the right and left common iliac arteries from the axis of the outlet segment of abdominal aorta), the developed model allowed to carry out a comparative study of the flow in healthy and stenosed branches.

The developed model was designed in the SolidWorks 2016 software package and made using 3D prototyping. The FLGPGR04 photopolymer was used for printing; this made it possible to study the flow using the ultrasonic Doppler method.

Numerical simulation and computational aspects

Numerical simulation of the flow in the given model of a segment of the vascular bed was performed assuming steady-state and laminar nature of the flow. We solved a complete system of Navier−Stokes equations for incompressible Newtonian fluid with constant viscosity.

The following fluid parameters were adopted: dynamic viscosity coefficient $\mu = 0.004$ Pa·s; density $\rho = 1050$ kg/m³. The flow rate $Q_{AA} = 4$ l/min was set at the inlet to the computational domain (this corresponds to maximum flow rate in the abdominal aorta within the cardiac cycle [5]); the flow rates at the outlets from the iliac arteries were set as follows:

0.8 l/min for right EIA,
1.44 l/min for left EIA,
1.04 l/min for left IIA;
zero pressure was set at the outlet from the right IIA.

The values and the ratios of the flow rates in the iliac arteries were selected for the healthy branch based on clinical data [5, 12]. No-slip conditions were imposed on the walls. The characteristic mean flow rates, vessel diameters, and the corresponding Reynolds numbers in the branches of the model are given in Table 1.

The computational domain was mainly covered with a quasi-structured mesh with hexahedral elements with five prismatic layers near the walls. The total number of cells in the

Reynolds number Re and mean flow velocities V_b in model branches

Vessel	Re	V_b, cm/s	D, mm
AA	1230	26	18
Right EIA	500	21	9
Right IIA	720	50	5.5
Left EIA	900	38	9
Left IIA	1040	72	5.5

N o t a t i o n : D is the diameter of the vessel. The names of the vessels are given in caption to Fig. 1.

mesh was about 3 million. The computational mesh was generated using the ICEM 16.2 program. The computations were performed using the ANSYS CFX 16.2 software package, with a second order accuracy of spatial discretization.

Experimental setup and measurement procedure

A setup with a fluid simulating blood circulating in it was assembled for experimental study of the flow structure in the given model. The setup consisted of two closed hydraulic circuits: a working circuit, where the model was installed, and an additional circuit used to fill the working hydraulic circuit with fluid. The experimental setup is shown schematically in Fig. 2.

Centrifugal pump 2 generates constant fluid flow in closed hydraulic circuit 1 at a rate Q = 4 l/min at the inlet to the abdominal aorta. Honeycomb 4, made of a straight tube 18 mm in diameter, with tubes 2 mm in diameter and 10 mm long glued inside it, is installed at the model inlet to suppress turbulence behind the pump and generate a uniform velocity profile. The flow rate is monitored using sensors 3 of electromagnetic flow meter, installed in front of the honeycomb 4, on the left external and on both internal iliac arteries. The following
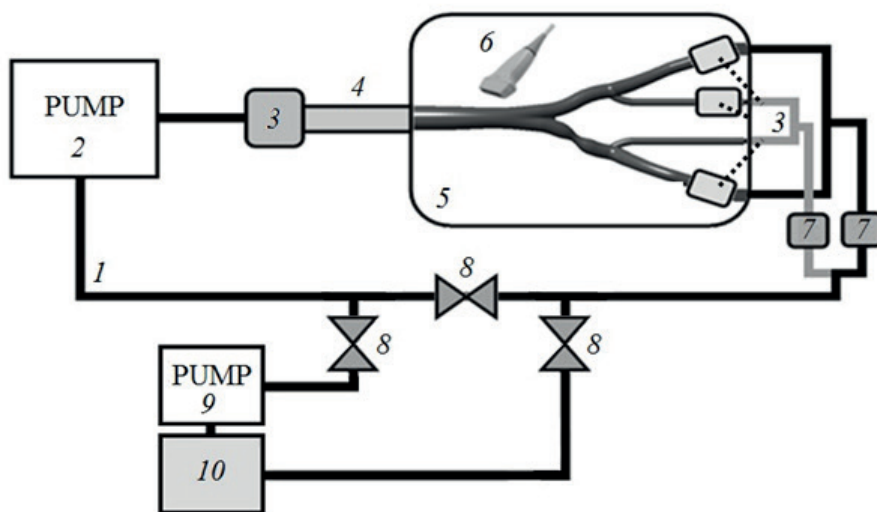

Fig. 2. Schematic of experimental setup:
closed hydraulic circuit 1; centrifugal and roller pumps 2 and 9; sensors 3 of electromagnetic flow meter; honeycomb 4; acoustic tray 5 with model of bifurcations of abdominal aorta and illiac arteries; sensor 6 of ultrasonic scanner; flow control valves 7; liquid drainage valves 8; container 10 with fluid simulating blood

flow rate ratios were set at the outlets from the healthy and stenosed branches using regulators 7:

$Q_{EIA}/Q_{IIA} = 1.1$ in the right branch;

$Q_{EIA}/Q_{IIA} = 1.4$ in the left branch,

which corresponds to the boundary conditions and the computational results.

The fluid simulating blood was a 36% aqueous glycerin solution with NaCl added (10 g/l), which is necessary for the sensor of the electromagnetic flow meter to operate. The density of the fluid was $\rho = 1050$ kg/m^3, the viscosity was close to the viscosity of blood and was $\mu = 0.004$ Pa·s.

An ultrasonic LogicScan 64 scanner, equipped with a linear transducer with an operating frequency of $5-7$ MHz, was used for measuring the velocity field in the model. The Doppler velocity spectrum was displayed on a computer screen in real time via the EchoWave II interface processing scanner signals. A suspension of gouache paint (5 g/l) was used as scattering ultrasonic particles.

Fields of axial velocity V_n and the projection of transverse velocity V_t on the axis of the ultrasonic sensor were visualized by color Doppler imaging. The ultrasonic sensor was installed at an angle of 60º to the vessel axis to measure the axial velocity, and at an angle of 90º to measure the transverse velocity projection. Shades of red, blue and gray are used as a scale for blood flow velocity in CDI. Red corresponds to the regions with velocities directed toward the sensor, blue to the velocities directed away from the sensor, gray to low velocities that cannot be reliably measured by the ultrasonic sensor.

Effect of stenosis on flow structure

Computations confirm that a complex vortex structure transforming along the vessel evolves in the given model of the bifurcation of the abdominal aorta and subsequent bifurcations of the iliac arteries. Fig. 3 shows the general picture of the streamlines. Apparently, regular structure of the flow changes considerably behind the stenosis. The positions and sizes of reverse flow regions are determined by the axial velocity fields (Fig. 4). A small region with reverse currents (negative velocities shaded in dark gray, occupying about 10% of the cross-sectional area) is observed behind the bifurcation of the common iliac artery in the branch without stenosis, disappearing at a distance of two calibers downstream.

Stenosis generates a separated region near the inner wall of the common iliac artery, persisting along the entire length of the external iliac artery. Separated regions do not form in the internal iliac arteries, regardless of whether there is stenosis upstream or not (Fig. 4).
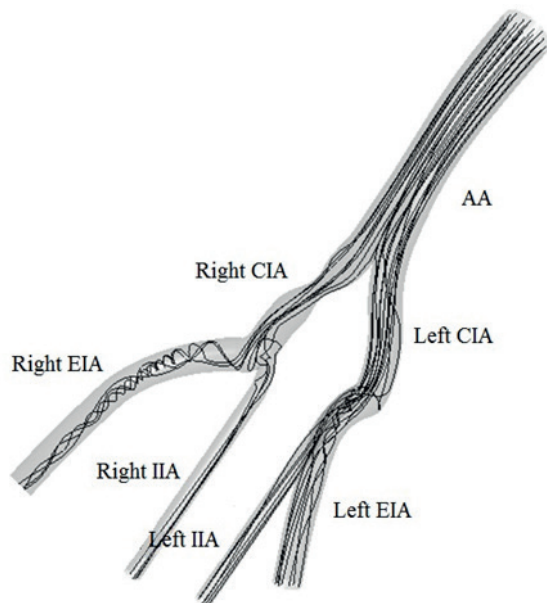

Fig. 3. Calculated streamlines in model of abdominal aortic bifurcation.
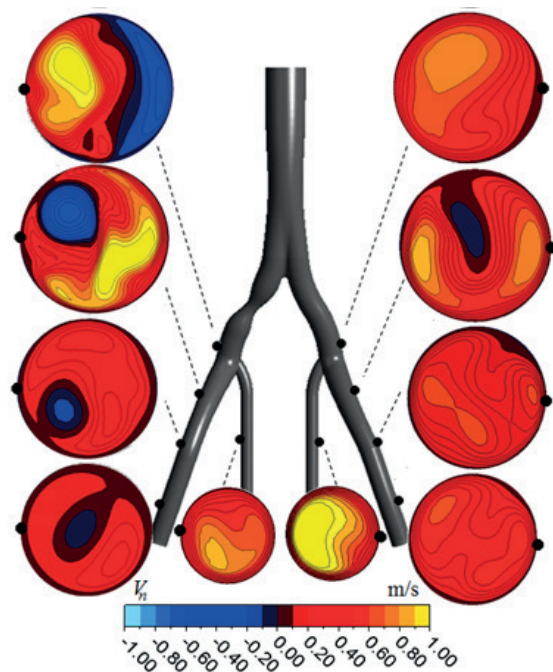Full names of the vessels are given in caption to Fig. 1

Fig. 4. Calculated effect of stenosis on axial velocity field V_n (m/s)
Scale of blood flow rate in vessel cross-sections: shades of red correspond to axial velocity directed toward the ultrasonic sensor, shades of blue to axial velocity directed away from the sensor, and dark shades to low velocities

Notably, there is a wide variety of vortex structures in the given model (Fig. 5, *a*, *b*).

Computations indicate that two-vortex flow evolves behind the bifurcation of the abdominal aorta in the common iliac arteries. Paired Dean vortices are detected in the branch without stenosis, after the first bifurcation in the common iliac arteries. The vortices are then transformed, generating four-vortex flow at the outlet from the given artery segment.

Two-vortex flow behind the stenosis is transformed into single-vortex, which persists along the entire length of the right external iliac artery.

Transitional flow from two-vortex to single-vortex forms at the outlet of the given segments of the internal iliac arteries; one of the vortices is considerably larger than the other.

Comparison of computational and experimental results

Computed fields of transverse velocity are compared with experimental results in Table 2. The table includes two types of data for the fields of transverse velocity projected onto the axis of the ultrasonic sensor: ultrasound images and computed fields constructed by the CDI scale of the ultrasound scanner. In addition, pictures of computed streamlines of transverse flow are given, allowing to determine the number, location, and shape of the vortices in several cross-sections of the model. The cross-sections compared show diverse vortex structures. The directions of transverse velocity projected onto the axis of the sensor are marked with arrows for each region in the ultrasound images. The sensor is located near the top of the ultrasound images.

The flow narrows in the convergent region in front of the bifurcation of the abdominal aorta; this is characterized by a two-color ultrasound image (cross-section *1*): here the region of negative projection of transverse velocity is closer to the sensor and the region of positive projection is further away from it.

Pronounced swirling flow evolving in the external iliac artery (in the stenosed branch) is characterized by a two-color ultrasound image (cross-section *2*), the boundary between these regions is approximately parallel to the axis of the ultrasonic transducer: the region with negative projection of transverse velocity (blue) is on the left, and the region with positive projection on the right (red).

Two-vortex flow (cross-section *3*) evolves after the bifurcation of the common iliac artery; it is characterized by a combination of several regions in the ultrasound image: positive
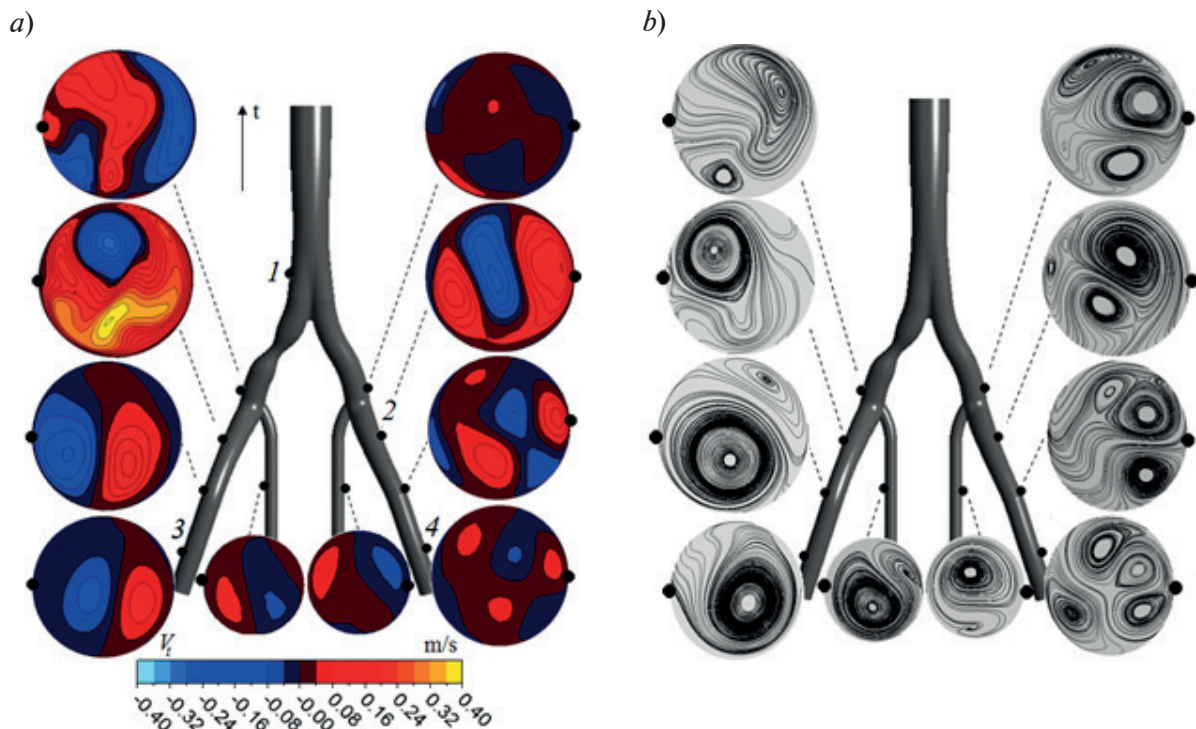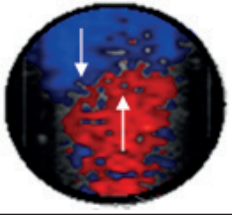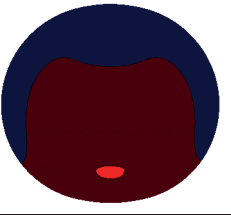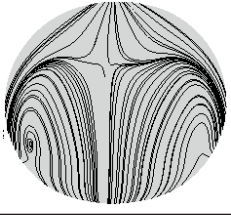
a) *b)*
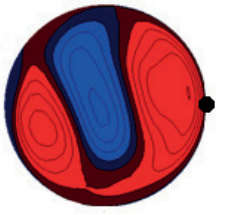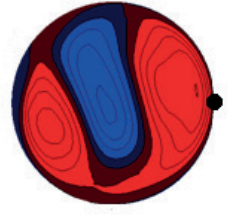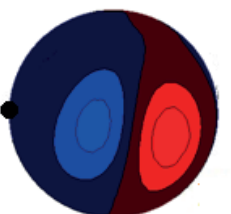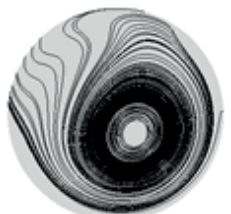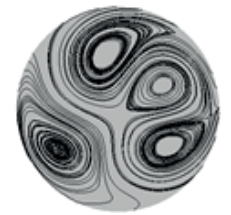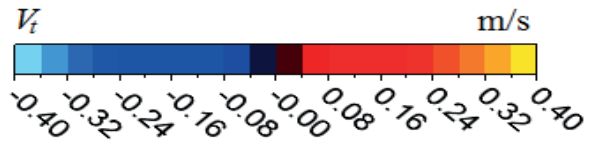
Fig. 5. Calculated effect of stenosis on structure of transverse flow:
isolines of velocity (*a*) and streamlines (*b*)
Numbers indicate the cross-sections comparing the calculated results in Table 2 with ultrasonic measurements

T a b l e 2

**Comparison of calculated and measured fields
of projected transverse velocity**

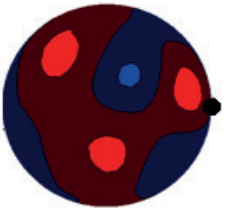| Cross-section	Field of transverse velocity projected on axis of ultrasonic sensor		Streamlines of transverse flow
	Result of ultrasound experiment	Computational result	
	Stenosed flow		
1			
	Two-vortex flow		
2			
	Single-vortex flow		
3			
	Four-vortex flow		
4			
	V_t m/s -0.40 -0.32 -0.24 -0.16 -0.08 -0.00 0.08 0.16 0.24 0.32 0.40		

N o t e . The locations of numbered cross-sections of the vessels are shown in Fig. 5.

projection on the left (red color), negative at the center (blue) and positive on the right (red)

Analysis of the data indicates that experimental results qualitatively agree with the computational results. Single vortex flow is clearly observed in ultrasound images. The picture becomes more complex if the number of vortices increases to two; the sizes of the region with positive projection of transverse velocity somewhat differ from the computational results. However, in general, the locations of the regions correspond to the computations. More complex flow formed by four vortices with low intensity (cross-section *4*) was difficult to detect by Doppler color imaging.

Conclusion

Numerical simulation and measurements by the ultrasonic Doppler method were used to obtain detailed information on the flow structure in a model including average bifurcation of the abdominal aorta, bifurcation of the common iliac arteries and segments of external and internal iliac arteries.

Two-vortex flow evolves in a spatially curved external iliac artery without stenosis, transforming into four-vortex flow downstream. Hemodynamically significant stenosis in the common iliac artery generates a separated region which is preserved along the entire length of the artery. Spatial bends of the external iliac artery after the stenosis generate swirling flow in the artery. Transitional flow from two-vortex to single-vortex forms at the outlet of the given segments of the internal iliac arteries; one of the vortices is considerably larger than the other.

Numerical modeling confirmed that ultrasound sensors can be used to detect one- and two-vortex structures of transverse flow in a spatial model of the vascular bed. In particular, the direction of rotation, the intensity and the position of the vortices can be determined by the ultrasound method.

REFERENCES

1. **Moore J.E., Ku D.N.,** Hemodynamics in the abdominal aorta: a comparison of *in vitro* and *in vivo* measurements, Journal of Applied Physiology. 76 (4) (1994) 1520−1527.

2. **Lee D., Chen, J.Y.,** Pulsatile flow fields in a model of abdominal aorta with its peripheral branches, Biomedical Engineering: Applications, Basis & Communications. 15 (5) (2003) 170−178.

3. **Long Q., Xu X.Y., Bourne M., Griffith T.M.,** Numerical study of blood flow in an anatomically realistic aorto-iliac bifurcation generated from MRI data, Magnetic Resonance in Medicine. 43 (4) (2000) 565−576.

4. **Lee D., Chen J.Y.,** Numerical simulation of steady flow fields in a model of abdominal aorta with its peripheral branches, Journal of Biomechanics. 35 (8) (2002) 1115−1122.

5. **Ke L., Wentao J., Yu C., et al.,** Fluid-solid interaction analysis on iliac bifurcation artery: a numerical study, international, Journal of Computational Methods. 16 (5) (2018) 1−18.

6. **Soares A.A., Gonzaga S., Oliveira C., et al.,** Computational fluid dynamics in abdominal aorta bifurcation: non-Newtonian versus Newtonian blood flow in a real case study, Computer Methods in Biomechanics and Biomedical Engineering. 20 (8) (2017) 1−10.

7. **Gataulin Y.A., Zaitsev D.K., Smirnov E.M., Yukhnev A.D.,** Structure of unsteady flow in the spatially curved model of the common carotid artery with stenosis: a numerical study, Russian Journal of Biomechanics. 23 (1) (2019) 58−66.

8. **Yukhnev A.D., Sinitsyna D.E.,** The blood vessel models: the technology development for making and following investigation, St. Petersburg State Polytechnic University Journal: Physics and Mathematics. (3(153)) (2012) 75−79.

9. **Gataulin Y.A., Zaitsev D.K., Smirnov E.M., et al.,** Weakly swirling flow in a model of blood vessel with stenosis: numerical and experimental study, St. Petersburg Polytechnical University Journal: Physics and Mathematics. 1 (4) (2015) 364−371.

10. **Lorbeer R., Grotz A., Durr M., et al.,** Reference values of vessel diameters, stenosis prevalence, and arterial variations of the lower limb arteries in a male population sample using contrast-enhanced MR angiography, PLoS One. 13 (6) (2018), e0197559. https://doi.org/10.1371/journal.pone.0197559

11. **Cuomo F., Roccabianca S., Dillon-Murphy D., et al.,** Effects of age-associated regional changes in aortic stiffness on human hemodynamics revealed by computational modeling, PLoS One. 12 (3) (2017) e0173177. https://doi.org /10.1371/journal.pone.0173177.

12. **Kurra V., Schoenhagen P., Roselli E.E., et al.,** Prevalence of significant peripheral artery disease in patients evaluated for percutaneous aortic valve insertion: preprocedural assessment with multidetector computed tomography, The Journal of Thoracic and Cardiovascular Surgery. 137 (5) (2009) 1258−1264.

13. **Shah P.M., Scartont H.A., Tsapogas M.J.,** Geometric anatomy of the aortic-common iliac bifurcation, Journal of Anatomy. 126 (Pt. 3) (1978) 451−458.

14. **O'Flynn P.M., O'Sullivan G., Pandit A.S.,** Geometric variability of the abdominal aorta and its major peripheral branches, Annals of Biomedical Engineering. 38 (3) (2010) 824−840.

15. **Yeung J.J., Jin Kim H., Abbruzzese T.A., et al.,** Aortoiliac hemodynamic and morphologic adaptation to chronic spinal cord injury, Journal of Vascular Surgery. 44 (6) (2007) 1254−1265.

THE AUTHORS

SINITSYNA Daria E.
Peter the Great St. Petersburg Polytechnic University
29 Politechnicheskaya St., St. Petersburg, 195251, Russian Federation
sinicina.daria@yandex.ru

YUKHNEV Andrey D.
Peter the Great St. Petersburg Polytechnic University
29 Politechnicheskaya St., St. Petersburg, 195251, Russian Federation
a.yukhnev@mail.ru

ZAITSEV Dmitrii K.
Peter the Great St. Petersburg Polytechnic University
29 Politechnicheskaya St., St. Petersburg, 195251, Russian Federation
zaitsev-aero@yandex.ru

TURKINA Maria V.
Peter the Great St. Petersburg Polytechnic University
29 Politechnicheskaya St., St. Petersburg, 195251, Russian Federation
turkinamaria@mail.ru

СПИСОК ЛИТЕРАТУРЫ

1. **Moore J.E., JR., Maier S.E., Ku D.N., Boensiger P.** Hemodynamics in the abdominal aorta: a comparison of *in vitro* and *in vivo* measurements // Journal of Applied Physiology. 1994. Vol. 76. No. 4 Pp. 1520−1527.

2. **Lee D., Chen J.Y.** Pulsatile flow fields in a model of abdominal aorta with its peripheral branches // Biomedical Engineering: Applications, Basis & Communications. 2003. Vol. 15. No. 5. Pp. 170−178.

3. **Long Q., Xu X.Y., Bourne M., Griffith T.M.** Numerical study of blood flow in an anatomically realistic aorto-iliac bifurcation generated from MRI data //Magnetic Resonance in Medicine. 2000. Vol. 43. No. 4. Pp. 565−576.

4. **Lee D., Chen J.Y.** Numerical simulation of steady flow fields in a model of abdominal aorta with its peripheral branches // Journal of Biome-chanics. 2002. Vol. 35. No. 8. Pp. 1115−1122.

5. **Ke L., Wentao J., Yu C., Xiaobao T., Zhihong Z., Ding Y.** Fluid-solid interaction analysis on iliac bifurcation artery: a numerical study // International Journal of Computational Methods. 2018. Vol. 16. No. 5. Pp. 1−18.

6. **Soares A.A., Gonzaga S., Oliveira C., Simxes A., Rouboa A.I.** Computational fluid dynamics in abdominal aorta bifurcation: non-Newtonian versus Newtonian blood flow in a real case study // Computer Methods in Biomechanics and Biomedical Engineering. 2017. Vol. 20. No. 8. Pp. 1−10.

7. **Гатаулин Я.А., Зайцев Д.К., Смирнов Е.М., Юхнев А.Д.** Структура нестационарного течения в пространственно-извитой модели общей сонной артерии со стенозом: численное исследование // Российский жур-

нал биомеханики. 2019. Т. 23. № 1. С. 69−78.

8. Юхнев А.Д., Синицына Д.Э. РазработА ка технологии изготовления и исследование моделей кровеносных сосудов // Научно-технические ведомости СПбГПУ. Физико-математические науки. 2012. № 3(153). С. 75−79.

9. **Гатаулин Я.А.,** Зайцев Д.К., Смирнов Е.М., Федорова Е.А., Юхнев А.Д. Расчетно-экспериментальное исследование слабозакрученного течения жидкости в модели кровеносного сосуда со стенозом // Научно-технические ведомости СПбГПУ. Физико-математические науки. 2015. № 4 (230). С. 36−47.

10. **Lorbeer R., Grotz A., Dᴜrr M., Vᴜlzke H., Lieb W., Kьhn J.-P., Mensel B.** Reference values of vessel diameters, stenosis prevalence, and arterial variations of the lower limb arteries in a male population sample using contrast-enhanced MR angiography // PLoS One. 2018. Vol. 13. No. 6. e0197559. https://doi.org/10.1371 /journal.pone.0197559

11. **Cuomo F., Roccabianca S., Dillon-Murphy D., Xiao N., Humphrey J.D. Figueroa C.A.** Effects of age-associated regional changes in aortic stiffness on human hemodynamics revealed by computational modeling // PLoS One. 2017. Vol. 12. No. 3. e0173177. https://doi.org/10.1371/journal.pone.0173177

12. **Kurra V., Schoenhagen P., Roselli E.E., et al.** Prevalence of significant peripheral artery disease in patients evaluated for percutaneous aortic valve insertion: preprocedural assessment with multidetector computed tomography // The Journal of Thoracic and Cardiovascular Surgery. 2009. Vol. 137. No. 5. Pp. 1258−1264.

13. **Shah P.M., Scartont H.A., Tsapogas M.J.** Geometric anatomy of the aortic-common iliac bifurcation // Journal of Anatomy. 1978. Vol. 126. Pt. 3. Pp. 451−458.

14. **O'Flynn P.M., O'Sullivan G., Pandit A.S.** Geometric variability of the abdominal aorta and its major peripheral branches // Annals of Biomedical Engineering. 2010. Vol. 38. No. 3. Pp. 824−840.

15. **Yeung J.J., Jin Kim H., Abbruzzese T.A., et al.** Aortoiliac hemodynamic and morphologic adaptation to chronic spinal cord injury // Journal of Vascular Surgery. 2007. Vol. 44. No. 6. Pp. 1254−1265.

СВЕДЕНИЯ ОБ АВТОРАХ

СИНИЦЫНА Дарья Эдуардовна − *аспирантка кафедры «Гидроаэродинамика, горение и теплообмен» Санкт-Петербургского политехнического университета Петра Великого.*
195251, Российская Федерация, г. Санкт-Петербург, Политехническая ул., 29
sinicina.daria@yandex.ru

ЮХНЕВ Андрей Данилович − з*аведующий учебной лабораторией кафедры «Гидроаэродинамика, горение и теплообмен» Санкт-Петербургского политехнического университета Петра Великого.*
195251, Российская Федерация, г. Санкт-Петербург, Политехническая ул., 29
a.yukhnev@mail.ru

ЗАЙЦЕВ Дмитрий Кириллович − *доктор физико-математических наук, профессор кафедры «Гидроаэродинамика, горение и теплообмен» Санкт-Петербургского политехнического университета Петра Великого.*
195251, Российская Федерация, г. Санкт-Петербург, Политехническая ул., 29
zaitsev-aero@yandex.ru

ТУРКИНА Мария Валерьевна − *студентка кафедры «Гидроаэродинамика, горение и теплообмен» Санкт-Петербургского политехнического университета Петра Великого.*
195251, Российская Федерация, г. Санкт-Петербург, Политехническая ул., 29
turkinamaria@mail.ru